Journal of Oceanography, Vol. 62, pp. 197 to 205, 2006

Current Structure and Volume Transport of the Soya Warm Current in Summer

Masaji Matsuyama[1]*, Makiko Wadaka[1], Taizo Abe[1], Masaaki Aota[2] and Yoshio Koike[1]

[1]*Faculty of Marine Science, Tokyo University of Marine Science and Technology, Konan, Minato-ku, Tokyo 108-8477, Japan*
[2]*Okhotsk Sea Ice Museum Hokkaido, Moto-Mombetsu, Mombetsu, Hokkaido 094-0023, Japan*

(Received 14 September 2005; in revised form 5 December 2005; accepted 6 December 2005)

ADCP, CTD and XBT observations were conducted to investigate the current structure and temperature, salinity and density distributions in the Soya Warm Current (SWC) in August, 1998 and July, 2000. The ADCP observations clearly revealed the SWC along the Hokkaido coast, with a width of 30–35 km and an axis of maximum speed of 1.0 to 1.3 ms^{-1}, located at 20–25 km from the coast. The current speed gradually increased from the coast to a maximum and steeply decreased in the offshore direction. The SWC consisted of both barotropic and baroclinic components, and the existence of the baroclinic component was confirmed by both the density front near the current axis and vertical shear of the alongshore current. The baroclinic component strengthened the barotropic component in the upper layer near the axis of the SWC. The volume transport of the SWC was 1.2–1.3 SV in August, 1998 and about 1.5 SV and July, 2000, respectively. Of the total transport, 13 to 15% was taken up by the baroclinic component. A weak southeastward current was found off the SWC. It had barotropic characteristics, and is surmised to be a part of the East Sakhalin Current.

Keywords:
· Soya Warm Current,
· barotropic current,
· baroclinic current,
· coastal boundary current,
· temperature front,
· density front,
· volume transport.

1. Introduction

The Soya Warm Current (referred to as SWC hereafter) is a typical coastal boundary current in the most southwestern part of the Sea of Okhotsk, flowing southeastward along the Hokkaido coast, Japan. The current is induced by the sea level difference between the Japan Sea and the Sea of Okhotsk, which shows a remarkable seasonal variation, being strong in summer and weak in winter (Aota, 1975; Ohshima, 1994; Matsuyama *et al*., 1999). The Soya Warm Current Water (SWCW) is characterized by high temperature and salinity in comparison with the surface and intermediate waters of the Sea of Okhotsk (IW). Its features can therefore often be seen in satellite sea surface temperature images as the strong contrast between the warm current water and the Sea of Okhotsk water (Fig. 1). The current has been considered to be mainly due to a barotropic flow since there is a weak density gradient across it (e.g., Aota, 1975; Takizawa, 1982). The current speed can thus not be estimated by indirect methods such as dynamical computation, and direct current measurements are required to clarify the current distribution in time and space. Two methods to measure the current have been used long-term measurement at moored stations, and radar or satellite-tracked buoys. The long-term current measurements at moored stations were limited to some points off Mombetsu (Aota and Kawamura, 1978, 1979) and off Sarufutsu (Aota and Matsuyama, 1987; Matsuyama *et al*., 1999). The current data obtained at the mooring stations indicated remarked seasonal variations. Tidal currents are not strong in the SWC region except near the Soya Strait along the Hokkaido coast, as evidenced by the current observations (Aota and Matsuyama, 1987; Odamaki, 1994) and numerical modeling (Kowalik and Polyakov, 1998). Radar buoy tracking has often been used to describe the surface current speed and its horizontal profile by using a land-based radar system (Aota, 1984). The surface buoy tracking results revealed a width of 30 to 40 km and a maximum speed of 0.6 to 1.0 ms^{-1} at 20 km from the coast.

The buoy tracking method cannot provide detailed horizontal and vertical synoptic descriptions of currents. The current measurements at moored stations near the main axis of the SWC during 25 hours displayed a slight

* Corresponding author. E-mail: masaji@s.kaiyodai.ac.jp

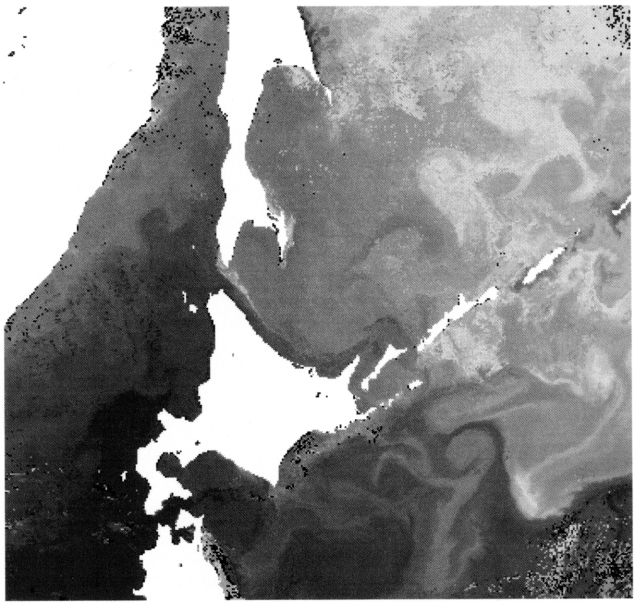

Fig. 1. NOAA infrared image on September 13, 1998 (from Website of Graduate School of Fisheries Science, Hokkaido University).

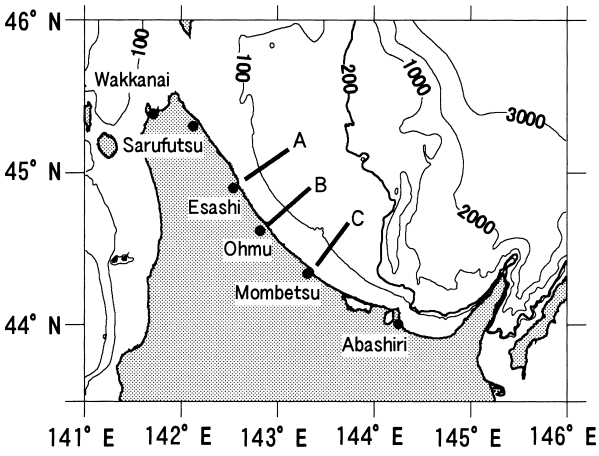

Fig. 2. Map of the observation area and locations of three observation lines. Bottom contours are in meters.

difference of the velocity between the upper and middle or lower layers (Aota, 1975), and the temperature and density distributions showed a weak gradient across the current (Aota, 1984). These observational results suggest the existence of a baroclinic current. Detailed observation of the current and its related thermal and salinity structure is therefore required to grasp the structure of the SWC.

In order to investigate the horizontal and vertical structure of the SWC, we conducted observations of current, temperature, and salinity distributions across the SWC using ADCP (Acoustic Doppler Current Profiler), CTD (Conductivity, Temperature and Depth) and XBT (Expendable Bathy-Thermography) deployed from the T/V Shin'yo-Maru, belonging to Tokyo University of Fisheries (the current Tokyo University of Marine Science and Technology). From the observational results, we report the current structure and volume transport estimated by ADCP in this paper. In addition, we discuss the characteristic of the flow observed off the SWC.

2. Observations and Data

The current data were obtained by the ship-mounted ADCP (RD Instrument Ltd., 150 kHz) one board T/V Shin'yo-Maru from 28 to 30 of August, 1998 and from 28 to 30 of July 2000 (Fig. 2). The ADCP instrument was set up with 4-m bin resolution from 12 m depth. The accuracy of the ADCP sensor is ± 3.8 cms^{-1}, according to the manufacturer's specification. Three observation lines, Line A (off Esashi), Line B (off Ohmu) and Line C (off Mombetsu), were taken across the SWC, as shown in Fig. 2. The presence of fishing gear from the coast to a few km from the coast along the Hokkaido coast unfortunately limited observations near the coast. From ADCP bottom tracking, it was possible to estimate velocity in the continental shelf region. The ship was held at a mean speed of 4.1 ms^{-1} (8 knot) and the ship position data were obtained with a differential Global Positioning System (DGPS). The current speeds were obtained by subtracting the ship speed from ADCP measurements. After the ADCP data were averaged every minute, i.e., a horizontal interval of about 250 m, the 5-minute running average data were obtained and used for the analysis.

The XBT measurements were also conducted in parallel with the ADCP measurements every 10 minutes (about 2.5 km interval). XBT data were used from 3 m depth, taking the adjustment time of a thermistor to the sea water into consideration. Conductivity, temperature, depth measurements were collected with CTD (Falmouth Scientific, Inc). The accuracy of the CTD sensor is ± 0.001°C in temperature, ± 0.0002 S/m in conductivity (about 0.002 in salinity), according to the manufacturer's specification. The accuracy, resolution and stability of the pressure sensor are 0.7 dbar, 0.028 dbar, and 0.14 dbar, respectively. The CTD measurements were made along Line C at about a 5 km interval in the summer of 2000. The time lag between the conductivity and temperature sensors for the CTD instrument was estimated as follows: after the response speed of the conductivity sensor was matched to that of the temperature, the data were cast into 5 m running mean to delete the noise and small scale variations and was converted into 1 m processed data. Salinity values obtained by the CTD measurements were calibrated with bottle sampled data.

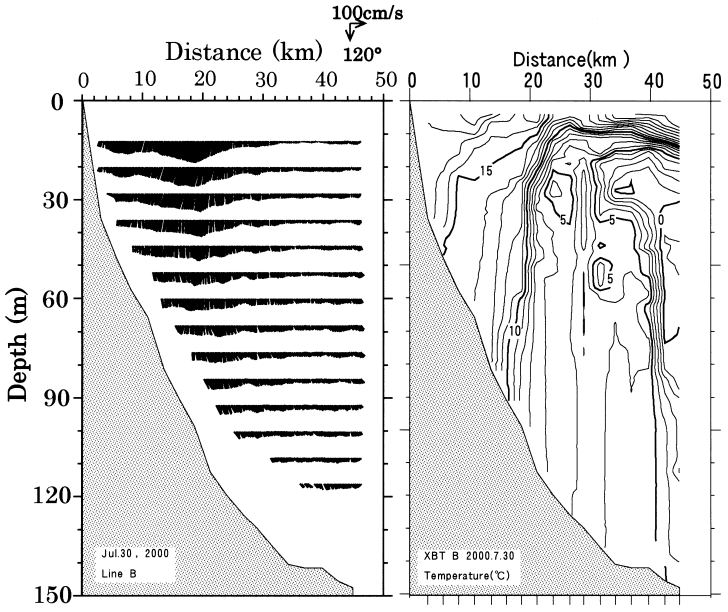

Fig. 3. Vertical section of current (left) and temperature (right) along Line B observed on July 30, 2000.

3. Results

3.1 Vertical sections of current and temperature

Figure 3 shows the current and temperature distributions every 8 m thickness along Line B observed on July 30, 2000. The remarkable current toward the direction of 120 degrees i.e., the alongshore current showing the SWC, existed though the water column from the coast to about 30 km. The location of maximum velocity was about 20 km from the coast and its value was over 1.2 ms^{-1}, corresponding to the SWC axis (Aota, 1984). The horizontal current profile was not symmetric about the jet axis. Rather, the current gradually increased from the coast to the maximum region and steeply decreased from the maximum in the offshore direction. Another weak peak existed in the surface layer around 10 km from the coast. The SWC gradually decreased with depth, and the vertical shear was large in the upper layer near the maximum current. In the region off 30 km, the current had a small speed, was uniform horizontally and had the same direction as the SWC. This current was 0.1 to 0.2 ms^{-1} in the middle and lower layers and was greater than in the surface layer.

The temperature distribution shows the existence of some fronts near 10 km, near 20 km and between 30 km and 40 km (offshore front). A sharp thermocline was formed from the sea surface to about 20 m depth offshore, 20 km from the coast. The temperature minimum at the sea surface appeared near 25 to 30 km from the coast, showing the cold water belt with a width of 10 km (Iida, 1962; Ishidu *et al*., 2005). Therefore the isotherms in the surface thermocline slightly descended in the offshore direction. The low temperature water was cut off from the offshore cold water mass and intruded into the warm water region. The strong temperature front near 20 km was found to be 6 to 14°C and conformed with the SWC axis seen in the current distribution. When the center of the temperature front is expressed as the 10°C isotherm, it inclined toward the coast from 22 km near the sea surface to 15 km near the bottom. The vertical shear in the current and temperature front near the current axis suggests that the SWC was composed not only of a barotropic component but also a baroclinic one.

The temperature front on the coast side was very weak, but it also agreed with the current peak in the surface layer near 10 km. On the other hand, the offshore front was complex with a temperature inversion in the middle layer, and was not found to correlate with the current. In summer, the SWCW (T > 7°C, S > 33.6) consisted of relatively warm water masses distributed from the coast to 30 km (Takizawa, 1982; Itoh and Oshima, 2000; Itoh *et al*., 2003). The southeastward current off about 30 km is thus considered to be less closely related to the SWC. The inclination of the surface thermocline in the offshore direction was consistent with the reduction of the southeastward current in the surface layer.

Figure 4 shows the current and temperature distributions along Line A obtained on July 30, 2000. The observation was made on the same day as Line B. The current and temperature distributions in the vertical section in Line A are similar to those in Line B shown in Fig. 3. Both current and temperature sections could be consid-

ered to have common properties between Line A and Line B, a distance of about 60 km.

Figure 5 shows the temperature, salinity and density distributions along Line C observed by the CTD observations on July 31, 2000. Figure 6 shows the T-S diagram based on these data. Two temperature fronts were also found near 20 km and 40 km corresponding to those seen in Figs. 3 and 4. The CTD observations were made at about a 5 km interval, so the temperature front was coarse in comparison with that obtained by the XBT observations shown in Figs. 3 and 4. The high temperature, saline water, i.e., the SWCW shown in Fig. 6, was distributed near the coastal region and the offshore water had low temperature and salinity (Intermediate Water). The salinity front existed only in the region from 30 to 40 km from the coast and inclined slightly from the sea surface to the bottom in the offshore direction. On the other hand, the density gradient existed only from 10 to 20 km, i.e., near the SWC axis. The temperature front agreed with the density one near the SWC axis, so the temperature front obtained by the XBT observations can be used to identify the density front and hence the existence of the baroclinic current in the upper layer near the main current axis.

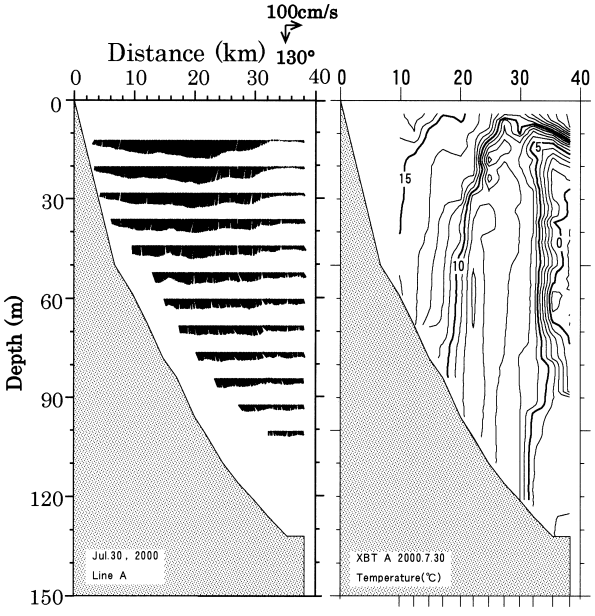

Fig. 4. As Fig. 3, but for Line A.

There was no density gradient in the region from 30 to 40 km from the coast where the salinity and temperature fronts were found. The front was 0 to 6°C in temperature and 33.0 to 33.8 in salinity on the line of sigma-t 26.6 to 26.7 (Fig. 6). In this region, the temperature gradient was sufficiently compensated by the salinity one, so no baroclinic current could be expected in this region. The offshore front distinguished the SWCW from the IW of the Sea of Okhotsk (e.g., Iida, 1962; Takizawa, 1982; Itoh and Ohshima, 2000), i.e., low temperature and low salinity water. The high temperature, low salinity water occupied the surface layer off the SWC and the isotherms inclined offshore, while the low temperature water was distributed under about 20 m depth to the sea bottom. The vertical distribution of current off the SWC shows a weak flow in the surface layer and an almost uniform flow in the layer below 30 m depth. These current and temperature distributions support the existence of the southeastward current with barotropic characteristics about 35 km from the coast. A temperature inversion is seen in some regions, but is confirmed to be canceled out by salinity,

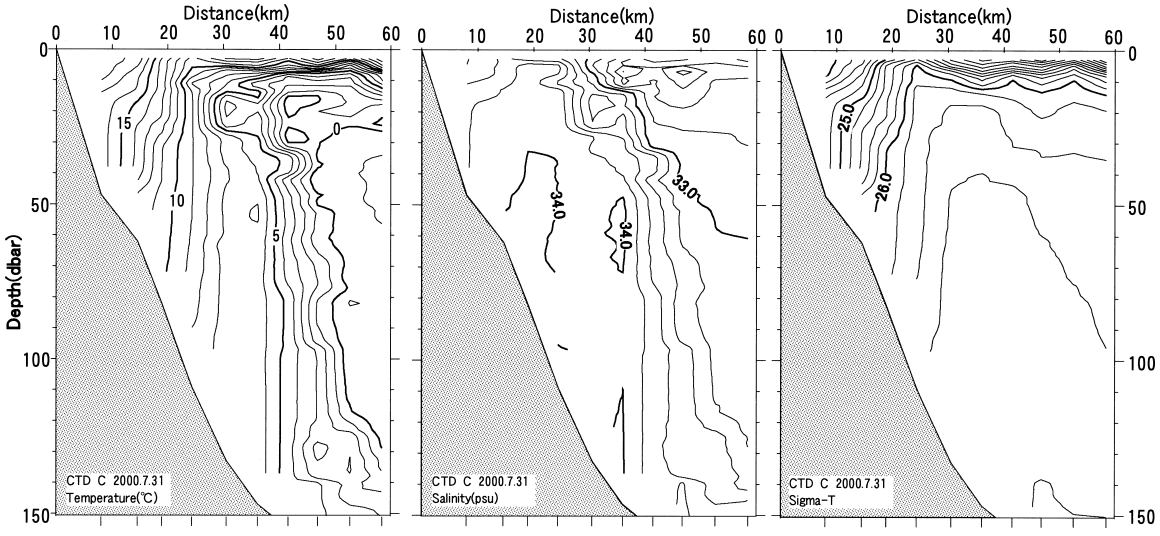

Fig. 5. Temperature (left), salinity (center) and density (right) distributions along Line C observed on July 31, 2000.

so the density is vertically stable (Aota, 1975; Takizawa, 1982; Itoh and Ohshima, 2000).

3.2 Baroclinic current

We extract the detailed characteristics of the horizontal current structure in both Line A and Line B, and compared them with each other. Figure 7 shows the alongshore current at 12 m depth, which is the uppermost depth of the ADCP observation, in both lines. The maximum current reaches 1.1 ms^{-1} at about 22 km from the coast in Line A and 1.3 ms^{-1} at about 20 km in Line B. The locations of the current axes are not very different from each other, but the current speed is enhanced downstream. The outer edge of the SWC can be estimated as 33 km in Line A but is less clear in Line B because the current does not have a zero-crossing. The SWC is seen to be confluent to the southeastward current in Line B. The minimum velocity existed in the region from 33 km to 40 km from the coast in Line B, so this region is considered to be the outer edge of the SWC. The currents again met a weak maximum at 13 km in Line A and 8 km in Line B in the inner region. These maxima agree with the temperature gradient of 15 to 17°C in the coastal region in Figs. 3 and 4.

The current and temperature distributions (Figs. 3 and 4) show the existence of baroclinic currents in the upper layer near the current axis at the same time, suggesting that the baroclinic current may play an important role in enhancing the current. To examine this idea further, we estimated the mean profiles of current and baroclinic velocity from the ADCP data. The baroclinic component existed near the current axis estimated from the temperature and current distributions, so the horizontal mean velocity between 15 km to 25 km from the coast is shown as a mean profile in Line A and Line B in Fig. 8. The profiles are obtained every 4 m vertically. The maxima of about 1.0 ms^{-1} appear at 12 m depth and are almost equal to each other. The mean velocity decreases with depth and becomes mostly constant at about 60 to 70 m depths, so we selected 60 m depth as the reference level of the baroclinic current. As a result, the constant velocity, i.e., barotropic velocity, is about 0.5 ms^{-1} around the current axis. The maximum velocity of the baroclinic component is about 0.5 ms^{-1} at 12 m depth, so the maximum is over this value at the sea surface.

The detailed structure of the baroclinic current along both lines can be estimated from the ADCP data by calculating the relative velocity. We selected 60 m depth as the reference level for the calculation of the baroclinic current. Figure 9 shows the baroclinic current referenced to 60 m depth. Some interesting features are found. Double peaks of positive velocity existed at 12 m depth, i.e., the highest peak at 22 km and a second peak at 14 km on Line A, and the highest peak at 19 km and a second peak at 7 km on Line B. These peaks are in very good agree-

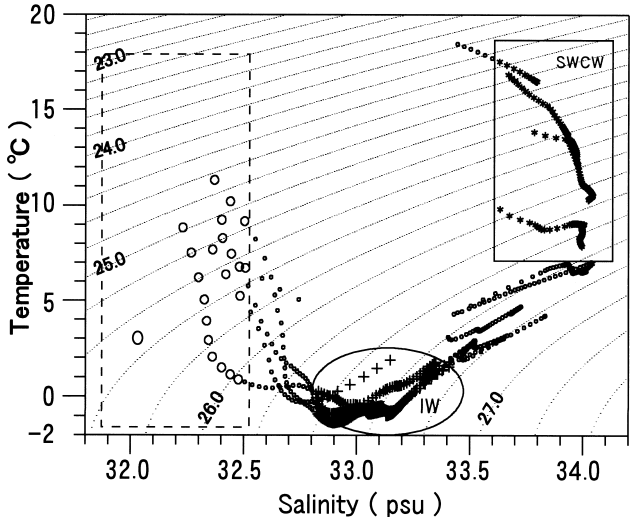

Fig. 6. T-S diagram for the data in Line C on July, 31, 2000. SWCW: Soya Warm Current Water. IW: Intermediate water of the Sea of Okhotsk.

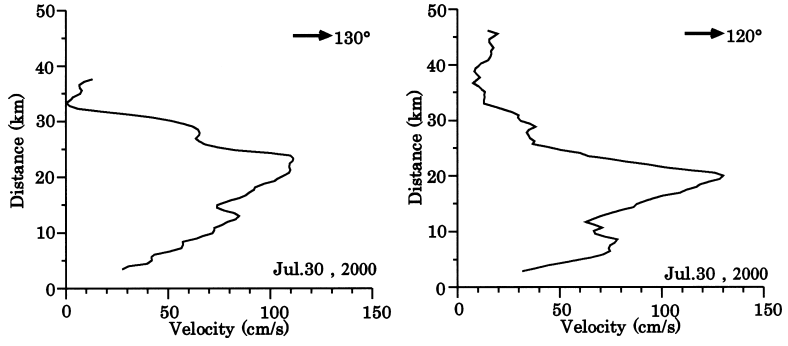

Fig. 7. Horizontal distributions of alongshore current at 12 m depth along Line A (left) and Line B (right).

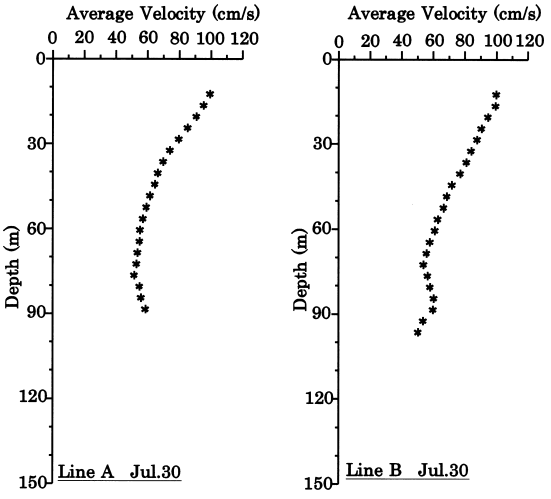

Fig. 8. Vertical profile of alongshore current averaged between 15 km and 25 km from the coast in Line A (left) and Line B (right).

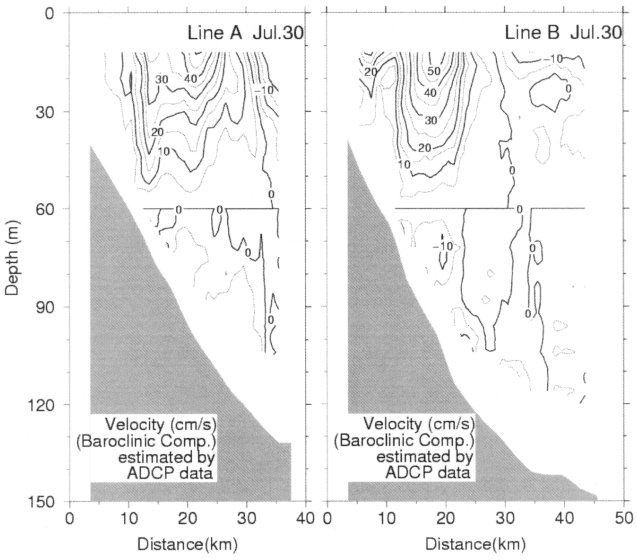

Fig. 9. Vertical sections of alongshore current referred to 60 m depth along Line A (left) and Line B (right) observed on July 30, 2000.

ment with the temperature front (Figs. 3 and 4). Moreover, in the offshore region of the SWC, the negative current in the surface layer only is seen, and no relative current lies under this layer in both lines. The surface negative current is related to the temperature gradient in the surface layer off the SWC in Figs. 3 and 4. The agreements between the current and temperature observations indicate the high credibility of the ADCP data in this observation.

In this study, the SWC is clearly shown by the ADCP and XBT observations to contain not only a barotropic component but also baroclinic component. In addition, the baroclinic current mainly existed in the upper layer above 60 m depth near the center of the SWC, 20 km from the coast. It plays a role in enhancing the SWC near the current axis when superposed on the barotropic component. Why has the baroclinic component in the SWC not been described previously? The baroclinic component seen here has a narrow width, like a front, as shown in Figs. 3 and 4, so it could not be discerned from the more broadly spaced observation stations across the SWC used in previous studies.

Recently, Itoh (2000) investigated the monthly mean cross section of the density cross the SWC off Hokkaido, and showed that the pycnocline inclines toward the coast during the period from May to October. This inclination of the pycnocline strongly supports the existence of the baroclinic current. Nakata *et al*. (2000) reported the temperature, salinity and density distributions with a significant baroclinicity from CTD observations across the Soya Strait in August, 1996. The baroclinic component of the SWC is stated to exist in the Soya Strait at the entrance of the Sea of Okhotsk.

4. Discussion

4.1 Estimation of volume transport of the SWC

The ADCP observations show the detailed current structure, both vertical and horizontal on Line A and Line B in both 1998 and 2000. It is possible to estimate the volume transport of the SWC across Line A and Line B using the ADCP data. The determination of the width of the SWC, i.e., the inner and outer boundaries, is required. The volume transport estimation strongly depends on the width, especially the location of the outer boundary. The current is at its shallowest and is weak near the coast, so the inner boundary is less of an influence on the volume transport estimation than the outer one. We estimate the width of the SWC as between the coast and 33 km for the outer boundary in 2000, from Figs. 3 and 4. On the other hand, in 1998, the outer boundary is about 30 km, judging from the current distribution in Fig. 10. We assume the coast to be the inner boundary and the current distribution near the coast is linearly extrapolated to no current at the coast. We estimate the baroclinic transport of the SWC in the same manner as the estimation of the baroclinic current in Fig. 9. The estimated volume transport is shown in Table 1.

The volume transport is estimated from the coast to 30 km from the coast by the ADCP data observed in 1998 (Table 1). The total, barotropic and baroclinic transports were almost equal between both lines, i.e., a total transport of about 1.3 SV, barotropic transport of over 1.0 SV and baroclinic transports of 0.2–0.3 SV. In the year 2000

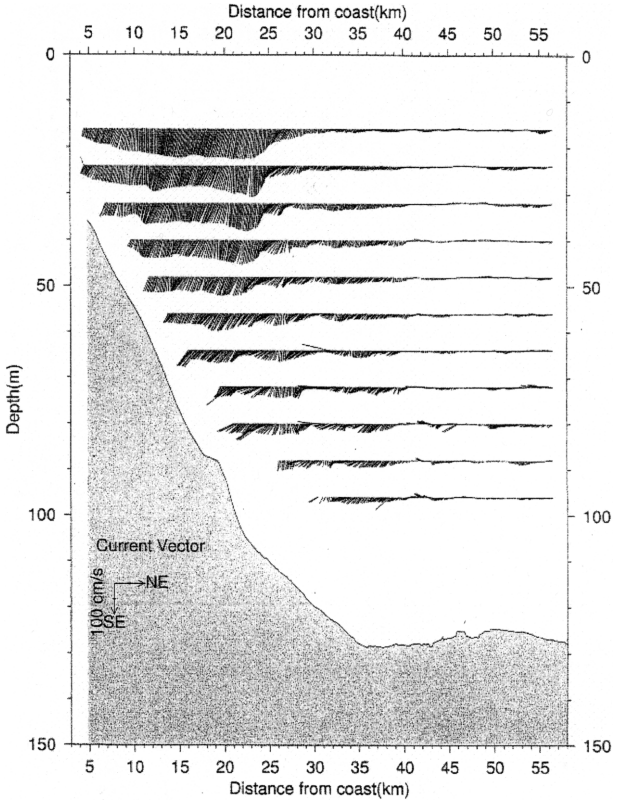

Fig. 10. Vertical section of current along Line A observed on August 27, 1998.

Table 1. Volume transport of the SWC.

	Total transport	Barotropic transport	Baroclinic transport
August, 1998			
Line A	1.31	1.06	0.25
Line B	1.29	1.08	0.21
July, 2000			
Line A	1.52	1.29	0.23
Line B	1.54	1.34	0.20

Unit: Sverdrup (10^6 m^3/s).

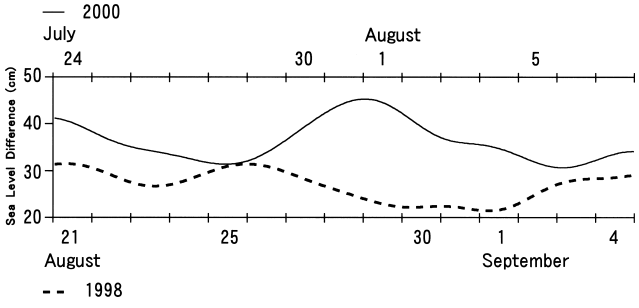

Fig. 11. Sea level difference between Wakkanai and Abashiri in July 1998 (broken line) and in August 2000 (full line).

observations, the total transport was 1.5 SV, the barotropic transport was 1.3 SV and baroclinic transport was 0.2–0.3 SV. Each transport obtained in 2000 was almost equal between both lines, too. The baroclinic volume transport was 13–15% of the total transport, so the SWC contains a baroclinic component, which is not large relative to the total volume transport. The estimated baroclinic transport was not different between both years, but the barotropic transport in the 2000 observations was larger than in the 1998 ones.

The difference of barotropic volume transport of between both years was 0.2 SV. The SWC is induced by the pressure difference, i.e., sea level difference between the Japan Sea and the Sea of Okhotsk (e.g. Aota, 1975). Thus the sea level difference between Wakkanai and Abashiri (Matsuyama *et al.*, 1999) is suitable to examine the current velocity of the SWC. Figure 11 indicates the sea level difference between both stations after removing the tidal fluctuations by using the tide killer filter (Thompson, 1983; Hanawa and Mitsudera, 1985). The records show that the sea level difference was larger in August 2000 than in July 1998, and the difference for two weeks ranged from 5 to 20 cm. The sea level difference between both stations is considered to induce the difference of the volume transport between both years. As a result, the width of the SWC in August 2000 (Fig. 3) is speculated to be wider than that in July 1998 (Fig. 10).

4.2 Southeastward barotropic current off the SWC

Recently, Ohshima *et al.* (2002) clearly showed that the East Sakhalin Current (Watanabe, 1963, hereafter ESC) flowed off the SWC using a satellite-tracked surface drifting overlaid with an AVHRR image, in October 1999. Mizuta *et al.* (2003) showed that the ESC was at a maximum in winter and in a minimum in summer using long term current measurements at the mooring stations off the Sakhalin east coast. In addition, the ESC is estimated to flow south along the east Sakhalin coast toward Hokkaido even in summer (Fig. 12). The relation between the SWC and the offshore ESC induced remarkable seasonal variations in sea level along the Hokkaido coast (Matsuyama *et al.*, 1999).

Figures 3, 4 and 9 indicate the weak southeastward current with a speed of near 0.1–0.2 cms^{-1}, having a characteristic of barotropic flow off the SWC, except the near sea surface. The weak southeastward flow is surmised to be a part of the ESC, but demonstrating this will require a more detailed investigation of the current.

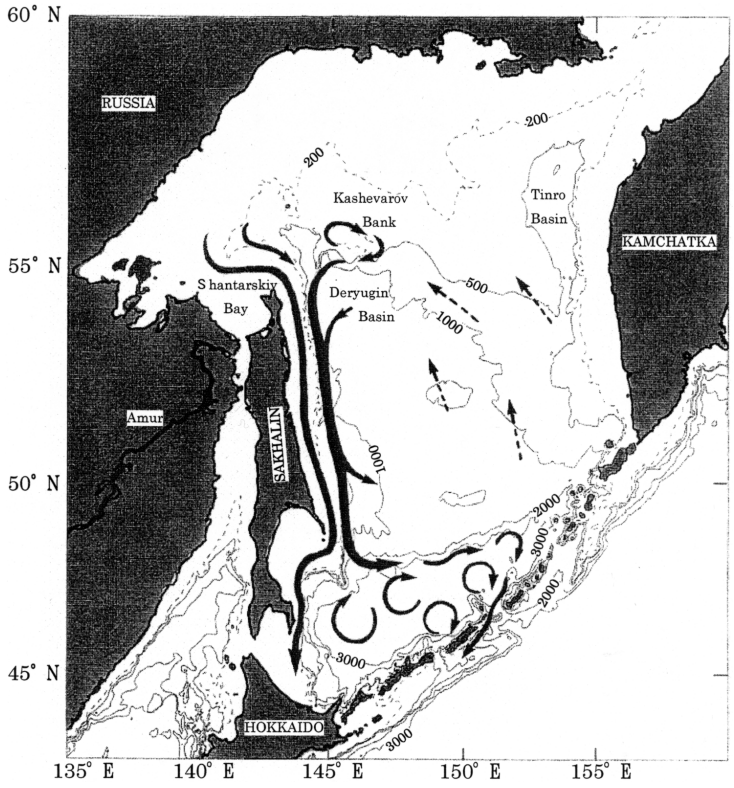

Fig. 12. Schematic view of the near surface circulation for the Sea of Okhotsk (after Ohshima *et al.*, 2002).

4.3 Possibility of tidal current influence

The ADCP observed current includes semidiurnal and diurnal tidal components. According to the observational results at a moored station near the Soya Strait off Sarufutsu reported by Aota and Matsuyama (1987), the diurnal current dominates the semidiurnal current because the amphidromic point is formed in the Soya Strait for the K_1 and O_1 constituents, but is not found for the semidiurnal constituents. The major axis of the tidal ellipse was, on average, obtained for K_1 of about 0.30 ms^{-1}, O_1 of 0.28 ms^{-1}, M_2 of 0.10 ms^{-1}, and S_2 of 0.04 ms^{-1} at the moored station off Sarufutsu (Aota and Matsuyama,1987). These values are almost the same order of magnitude as the SWC near the Soya Strait, so it is not negligible for the estimation of the SWC. Odamaki (1994) indicated that the tidal currents were much lower than the SWC current except around the Soya Strait, from the tidal currents obtained at some moored stations along the Hokkaido coast in the Sea of Okhotsk. He reported the tidal current amplitudes at two stations about 7 km and 20 km from the coast in Line A (Fig. 2). The K_1 and O_1 amplitudes are not very different between both stations, viz., 0.08 ms^{-1} and 0.07 ms^{-1}. In addition, the current amplitudes of M_2 and S_2 constituents have magnitudes of 0.02 to 0.04 ms^{-1} at both onshore and offshore stations. He also obtained the tidal current amplitudes at two stations of about 3 km and 40 km in Line B, which have a magnitude of 0.06 to 0.07 ms^{-1} for K_1 and O_1 constituents and less than 0.04 ms^{-1} for M_2 and S_2 constituents at both stations. The current observations in July 2000 were made during the spring tide for the diurnal period, so the tidal current is supposed to reach about 0.15 ms^{-1} in Line A and 0.13 ms^{-1} in Line B instantaneously. The tidal current's effects on the SWC distribution are minor except near the Soya Strait, so we neglect the influence of tidal current in our analysis of the SWC in Line A and Line B as a first approximation.

5. Conclusion

ADCP and XBT observations were conducted to investigate the current structure and the temperature, salinity and density distributions in the Soya Warm Current (SWC) in August, 1998 and July, 2000.

The ADCP data clearly show the southeastward current along the Hokkaido coast, revealing the SWC with a width of 30–35 km and current axis located 20–25 km from the coast. The maximum velocity was 1.0 to 1.3 ms^{-1} near the sea surface. The horizontal current speed gradually increased from the coast to a maximum and steeply decreased in the offshore direction. The SWC

consisted of both barotropic and baroclinic currents, and the existence of the baroclinic current was confirmed by both the density front near the current axis and vertical shear of the alongshore current. The baroclinic current strengthened the barotropic current in the upper layer near the center of the SWC. The velocity near the center decreased with depth and became mostly constant at about 60 to 70 m depth. When 60 m depth is selected as the reference level of the baroclinic current, the barotropic velocity was about 0.5 ms^{-1} and the maximum velocity of the baroclinic component at 12 m depth was about 0.5 ms^{-1} around the current axis, averaged between 15 km to 25 km from the coast. The volume transport in the region from the coast to 35 km offshore was 1.2–1.3 SV and about 1.5 SV in August, 1998 and July, 2000, respectively. Of total transport, 10 to 15% was carried by the baroclinic component. A weak southeastward current was found off the SWC. It had barotropic characteristics, and is considered to be a part of East Sakhalin Current.

Acknowledgements

We are deeply indebted to the crew of T/V Shin'yo-Maru of Tokyo University of Marine Science and Technology, and to Dr. Y. Kawamura and Mr. K. Ogawa for their supports in the observations. Thanks are extended to Drs. J. Yoshida and Y. Kitade for their helpful comments. The authors are grateful to the three anonymous reviewers for useful comments and suggestions.

References

Aota, M. (1975): Studies on the Soya Current. *Low Temp. Sci., (Ser. A)*, **33**, 151–172 (in Japanese).

Aota, M. (1984): Oceanographic structure of the Soya Warm Current. *Bull. Coast. Oceanogr*., **22**, 30–39 (in Japanese).

Aota, M. and T. Kawamura (1978): Observation of oceanographic condition in the Sea of Okhotsk coast of Hokkaido in winter. *Low Temp. Sci., (Ser. A)*, **37**, 93–105 (in Japanese).

Aota, M. and T. Kawamura (1979): Observation of oceanographic condition in the Sea of Okhotsk coast of Hokkaido in winter II. *Low Temp. Sci., (Ser. A)*, **38**, 135–142 (in Japanese).

Aota, M. and M. Matsuyama (1987): Tidal current fluctuations in the Soya Warm Current. *J. Oceanogr. Soc. Japan*, **43**, 276–282.

Hanawa, K. and H. Mitsudera (1985): On the data processing of daily mean values of oceanographical data. *Bull. Coast. Oceanogr*., **23**, 79–87 (in Japanese).

Iida, H. (1962): On the water mass in the central region of the South-Western Okhotsk Sea. *J. Oceanogr. Soc. Japan*, **20th Anniversary Vol**., 272–278.

Ishidu, M., Y. Kitade and M. Matsuyama (2005): Formation mechanism of the cold water belt formed off the Soya Warm Current. *J. Oceanogr*. (submitted).

Itoh, M. (2000): Formation and distribution of Okhotsk Sea Intermediate Water. Doctor Dissertation, Hokkaido University, 62 pp.

Itoh, M. and K. I. Ohshima (2000): Seasonal variations of water masses and sea level in the southern part of the Sea of Okhotsk. *J. Oceanogr*., **56**, 643–654.

Itoh, M., K. I. Ohshima and M. Wakatsuchi (2003): Distribution and formation of Okhotsk Sea Intermediate Water; an analysis of isopycnal climatology data. *J. Geophys. Res*., **108**(C8), 3258, doi:10.1029/2002JC001590.

Kowalik, Z. and I. Polyakov (1998): Tides in the Okhotsk Sea. *J. Phys. Oceanogr*., **28**, 1389–1409.

Matsuyama, M., M. Aota, I. Ogasawara and S. Matsuyama (1999): Seasonal variation of Soya Current. *Umi no Kenkyu*, **8**, 333–338 (in Japanese with English abstract).

Mizuta, G., K. I. Ohshima, Y. Fukamachi and W. Wakatsuchi (2003): Structure and seasonal variations of the East Sakhalin Current. *J. Phys. Oceanogr*., **33**, 2430–2445.

Nakata, A., I. Tanaka, H. Yagi, T. Watanabe, G. A. Kantakov and A. D. Samatov (2000): Formation of high-density water (over 26.8 sigma-t) near the La Perous Strait (the Soya Strait). *Proc. of the Second PICES Workshop on the Okhotsk Sea and Adjacent Areas*, 145–147.

Odamaki, M. (1994): Tides and tidal currents along the Okhotsk coast of Hokkaido. *J. Oceanogr*., **50**, 265–279.

Ohshima, K. I. (1994): The flow system in the Japan Sea caused by a sea level difference through shallow straits. *J. Geophys. Res*., **99**(C5), 9925–9940.

Ohshima, K. I., M. Wakatsuchi, Y. Fukamachi and G. Mizuta (2002): Near-surface circulation and tidal currents of the Sea of Okhotsk observed with the satellite-tracked drifters. *J. Geophys. Res*., **107**(C11), 3195–3210.

Takizawa, T. (1982): Characteristics of the Soya Current in the Okhotsk Sea. *J. Oceanogr. Soc. Japan*, **38**, 281–292.

Thompson, R. O. R. Y. (1983): Low-pass filters to suppress inertial and tidal frequencies. *J. Phys. Oceanogr*., **13**, 1077–1083.

Watanabe, K. (1963): On the reinforcement of the East Sakhalin Current preceding to the sea ice season off the coast of Hokkaido—study on sea ice in the Okhotsk sea (IV). *Oceanogr. Mag*., **14**, 117–130.